

# Anklebot-Assisted Locomotor Training After Stroke: A Novel Deficit-Adjusted Control Approach

Anindo Roy, *Senior Member, IEEE*, Hermano I. Krebs, *Senior Member, IEEE*, Joseph E. Barton, *Member, IEEE*, Richard F. Macko, and Larry W. Forrester

**Abstract**—In this paper, we present an approach to using the impedance-controlled “anklebot” for task-oriented locomotor training after stroke. Our objective is to determine the feasibility of using the anklebot as a gait training tool by increasing the contribution of the paretic ankle in walking function. Underlying our training approach is a novel gait event-triggered, sub-task control algorithm that enables precise timing of robotic assistance to key functional deficits of hemiparetic gait, as well as sagittal-plane biomechanical models capable of predicting necessary levels of robotic support specific to the nature and severity of deficits. These features may facilitate customizability of assisted walking to individual gait deficit profiles. As with our previous studies, we employ an adaptive approach in that, training parameters are incrementally progressed towards those of more normal gait depending on subject performance and tolerance. Here, we present and validate the sub-event detection and sub-task control method, the biomechanical models for the swing and landing phases of gait, and as proof-of-concept, pilot data to demonstrate initial efficacy of the approach.

## I. INTRODUCTION

STROKE is the leading cause of long-term disability in the United States and its prevalence will increase with an aging population [1]. The impact on walking is significant, negatively affecting an individual’s mobility [2] and ability to perform everyday activities, including optimal participation in community life.

Physical therapy remains the standard of care to retrain patients and restore walking ability, but many individuals still have residual deficits, even after completion of all conventional rehabilitation therapy. Moreover, increasing clinical and experimental data suggest that conventional

rehabilitation does not provide adequate task-repetitive practice to optimize motor learning and recovery across the continuum of care. This has prompted the development and utilization of robotic tools for delivering movement therapy. The prevailing rationale is that robots lend themselves to the process of motor learning (ML) by facilitating massed repetitive practice, providing precise measurement capability and the potential to customize training progression and ML paradigms.

The US Department of Veterans Affairs Baltimore Medical Center (VAMC), in collaboration with MIT, has developed an impedance-controlled, highly backdriveable, 2 degree-of-freedom (DOF) actuated ankle robot (“anklebot”) to improve walking and balance functions after stroke [3]. The rationale to focus on the ankle was due to the critical role it plays in the biomechanics of gait and balance. For example, the ankle musculature provides propulsion during mid-to-late stance, ground clearance during swing, and “shock absorption” during the landing phase of gait. Following a stroke, some (or all) of these ecological aspects of gait are disrupted. For example, “drop foot” is a common impairment caused by a weakness in the dorsiflexor muscles that lift the foot. A major complication of drop foot is the slapping of the foot after heel strike (foot slap). In addition to inadequate dorsiflexion (DF), the paretic ankle may also suffer from excessive inversion. This begins in the swing phase and results in toe contact (as opposed to heel contact) and lateral instability in stance. The anklebot possesses the potential to control both since it can be actuated in 2-DOFs [3], and is able to independently modulate stance, swing, and specific sub-tasks within the gait cycle to better address the heterogeneity of hemiparetic (HP) stroke recovery.

The work presented here is part of a larger ongoing study at the Baltimore VAMC that investigates the hypothesis that a modular, deficit-adjusted approach to using the impedance-controlled anklebot for task-oriented locomotor training will lead to sustainable gains in mobility function in those with residual HP gait deficits. The underlying rationale is the need to promote volitional control of the paretic leg through versatile interaction during robot-assisted gait—one that does not impose prescribed movement as a substitute for volitional control, but rather responds to disparate forms and degrees of impairments with the ability to dynamically adjust the level of support concomitant with the patient’s capacity and recovery. Our *overall* objective is to determine whether sensorimotor task-oriented practice in walking with

Manuscript received September 17, 2012, accepted January 7, 2013. This work was supported by the Department of Veterans Affairs (VA) RR&D Service grant B2294T and the Baltimore VA Medical Center grant B3688R. H.I. Krebs is supported by NIH grant 1R01HD069776-01A1. L.W. Forrester is supported by VA RR&D Merit Pilot grant RX000351-01.

A. Roy is with the Dept. of Neurology, University of Maryland at Baltimore (UMB) and the Baltimore VA Medical Center (VAMC), Baltimore, MD 21201, and the Dept. of Bioengineering, University of Maryland at College Park, College Park, MD 20742, USA (phone: 410-637-3241; fax: 410-605-7913; e-mail: [ARoy@som.umaryland.edu](mailto:ARoy@som.umaryland.edu)).

H.I. Krebs with the Dept. of Mechanical Engineering, Massachusetts Institute of Technology, Cambridge, MA 01239 (email: [hikrebs@MIT.edu](mailto:hikrebs@MIT.edu)).

J.E. Barton is with UMB Dept. of Neurology and the Baltimore VAMC, Baltimore, MD 21201 USA (e-mail: [JBarton@som.umaryland.edu](mailto:JBarton@som.umaryland.edu)).

R.F. Macko is with UMB Dept. of Neurology, the Geriatric Research Education and Clinical Core, and the Baltimore VAMC, Baltimore, MD 21201 USA (email: [rmacko@grecc.umaryland.edu](mailto:rmacko@grecc.umaryland.edu)).

L.W. Forrester is with UMB Dept. of Physical Therapy and Rehabilitation Science and the Baltimore VAMC, Baltimore, MD 21201 USA (e-mail: [LForrester@som.umaryland.edu](mailto:LForrester@som.umaryland.edu)).

precisely-timed and appropriately-scaled robotic support delivered to the paretic ankle at critical instances of the gait cycle, can improve key functional deficits of HP gait. As a first step, here we present a novel control approach for safe, effective first use of anklebot-assisted treadmill (TM) gait training in those with HP gait deficits: 1) a control algorithm that enables precise sub event-triggered robotic support during the gait cycle; 2) sagittal-plane biomechanical models for swing and landing phases of gait to scale robotic support to deficit profiles; and 3) proof-of-concept by validating the control algorithm and biomechanical models during anklebot-assisted TM walking; first, with a healthy participant and then, with a chronic stroke survivor.

## II. OVERVIEW OF CURRENT GAIT TRAINING APPROACHES

In conventional gait physiotherapy, the therapist pushes or slides the patient's swing leg forward, either on the ground or on a TM. There is clear evidence from recent studies (e.g., [4]) that higher intensities of walking practice (resulting in more trained repetitions) result in better outcomes for patients after stroke; however, one disadvantage of TM-based therapy might be the necessary effort required by therapists to set the paretic limbs and to control weight shift, thereby possibly limiting the intensity of therapy especially in more severely disabled patients. To counter this problem, in the past decade and a half, several groups have designed and deployed automated electromechanical devices that provide non-ambulatory patients intensive practice of complex gait cycles, thereby reducing therapist effort compared to TM training with partial body weight support alone. Most of these devices fall in one of two categories based on their principle of operation: 1) The leg is propelled by the robotic exoskeleton orthosis acting on the patient's leg (e.g., [5]), or 2) Actuated foot plates are attached to the patients' foot simulating phases of gait (e.g., [6]). More recent devices include "Haptic Walker" [7], lower extremity powered exoskeleton (LOPES) [8], and MIT-Skywalker [9].

## III. SEATED COMPUTER-VIDEO INTERFACED ANKLEBOT INTERVENTIONS: AN IMPAIRMENT-FOCUSED APPROACH

To date, we have studied the effects of anklebot mass on HP gait kinematics [10], demonstrated its safety and feasibility for use in chronic stroke, and its use as a clinical assessment tool in the measurement of passive ankle stiffness (PAS) [11]—a potential marker related to motor deficit severity. Clinical investigations using seated computer-video interfaced anklebot training in chronic HP stroke provided evidence of paretic ankle ML, both in the short-term (48-hours) [12] and at 6 weeks [13]. Specifically, chronic stroke survivors who underwent 6 weeks of seated anklebot training with their paretic ankle engaged in a visuomotor task customized to individual ankle deficits, showed reduced ankle impairments (increased strength, voluntary range of motion), improved paretic ankle motor control (smoother and faster ankle movements), and higher unassisted overground (OG) gait speed [13]. Notably, the

mean increase (20%) in independent floor-walking speed after 6 weeks of seated anklebot training is comparable to that reported for other task-specific, locomotor training approaches in the chronic stroke population (e.g., [14]). These findings resulting from seated anklebot intervention support a rationale for a modular, impairment focused approach towards upright anklebot training.

## IV. THE ANKLEBOT AS A GAIT TRAINING DEVICE

### A. Clinical considerations

The anklebot must be capable of delivering tailored therapies in order to address the wide variety of gait deficits and compensatory gait strategies encountered in the clinic. From a control standpoint, its closed loop must also be Hurwitz stable to ensure stability of the man-machine interface. Both these issues can be addressed, at least in part, by taking advantage of the anklebot's 2-DOF actuation [3], its impedance control, and the sub-event triggered timing algorithm that we have developed (*see* IV-B). The 2-DOF actuation enables customization of robotic support to different profiles of HP gait deficits in the sagittal and/or frontal planes, while impedance control makes the robot minimally intrusive by providing assistance "as-needed" i.e., allowing and encouraging volitional movements much like a therapist, rather than constraining the natural leg dynamics. Stability is addressed along with the question of when and how much robotic support to provide during assisted walking across a wide range of HP gait deficit profiles.

### B. The timing issue: A gait sub-event triggered solution

We prioritize precise timing of robotic support at critical gait sub-events of interest in order to both prevent destabilization and afford a deficit-adjusted approach. Accordingly, we developed a sub event-triggered method (Fig. 1) in which the anklebot delivers torques at the paretic ankle during one or more of two key time epochs, each with unique functional needs: (1) Concentric plantar flexion (PF) torque to enable push-off propulsion during terminal stance (TS), starting with heel-off and peaking just prior to toe-off (*see* accompanying Video); (2) Concentric DF torque to facilitate swing clearance, starting at toe-off and continuing

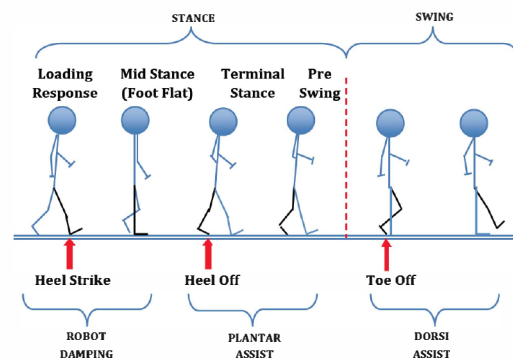
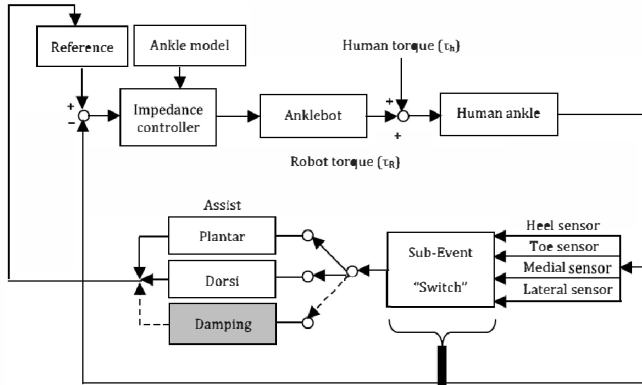


Fig. 1. Conceptual diagram showing three key sub-events during a gait cycle. Depending on the type of gait deficit(s), the anklebot is programmed to generate assistive (or resistive) torques at the paretic ankle during one or more gait sub-events.

until mid-swing; and (3) Velocity-dependent viscous (resistive) torque to attenuate or absorb the impact force at landing. Both assistive and resistive torques are generated by kinematic control of the anklebot i.e., by having the total net torque (human plus robot) track an appropriate positional reference trajectory. The impedance controller generates ankle torques proportional to the magnitude of the positional error between the commanded and actual ankle trajectory via the torsional stiffness ( $K$ ) and damping ( $b$ ) settings (Fig. 2). Notably, we are not explicitly controlling the torque output (i.e., force control) nor the position (i.e., position control) to actuate the anklebot.



Gait Event	Heel Footswitch		Toe Footswitch		Medial Footswitch		Lateral Footswitch		Torque Assist
	on	off	on	off	on	off	on	off	
Heel Strike	X		X		X		X		Resistive damping
Foot Flat	X		X		X		X		None
Heel Off		X	X		X		X		Plantar
Toe Off		X		X		X		X	Dorsi

Fig. 2. Conceptual block diagram showing the sub event-triggered approach to detect gait sub-events of interest and precisely time robot actuation. In the figure, the sub-event of interest (shown for illustration) is landing or heel strike (dashed line). Biomechanical models specific to each phase of interest are used to scale robotic torques to deficit severity via the controller settings,  $K$  and  $b$  (see Section V for details).

In order to precisely time robotic support, we employed footswitches embedded inside the individual’s shoes to detect the occurrence of key gait sub-events. Although not novel in itself (e.g., [15]), this approach is effective, at least in principle, because it allows the human to “inform” (via 5-pin LEMO footswitch insoles worn bilaterally) the anklebot of the occurrence of gait sub-events, thereby enabling accurate and automatic adjustment of timing of robotic outputs across strides. Each footswitch (B&L Engineering, Santa Ana, CA) contains 4 individual switches: at the heel, forefoot, medial and lateral zones at the level of metatarsals. An event is detected when the cumulative footswitch voltage equals a pre-defined value unique to each sub-event (Fig. 3). For example, heel-strike is detected when all switches except the heel switch are open. Following this, the loading continues and is characterized by the closing of medial-lateral switches followed by the forefoot switch at which point the foot is in mid-stance. Late stance is detected by the opening of the heel switch followed by the medial-lateral

switches marking the beginning of terminal stance. The forefoot switch then opens marking the beginning of swing phase. For optimal sensitivity, tolerance bands were created around each sub-event’s threshold voltage, then calibrated to ensure consistent, accurate capture of each sub-event. It is possible, especially during the early phases of therapy, that the ipsilateral (affected, robot donning) footswitch may not detect sub-events and actuate the anklebot with sufficient precision; to counter this, we have developed capacity to achieve this using the contralateral (unaffected) footswitch.

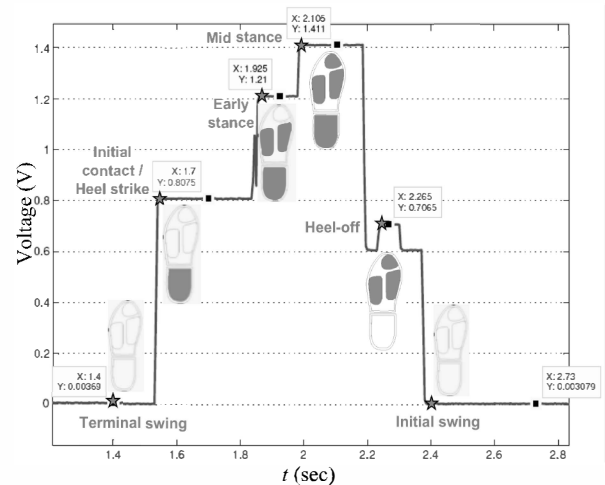


Fig. 3. Footswitch voltages during a typical gait cycle. Shaded regions within the footprints represent instants when one or more switches close due to the occurrence of a gait sub-event (filled asterisks).

### C. Performance metrics: Timing of robotic assist

In order to quantify and validate the accuracy of sub-event detection, we devised the following metrics:

1) Uniqueness ( $U$ ) is the number of robot torque pulses across gait cycles, i.e.,

$$U = |N_{\text{cycle}} - N_{\text{single,torque}}| \quad (1)$$

where  $N_{\text{cycle}}$  is the number of gait cycles and  $N_{\text{single,torque}}$  is the number of gait cycles that consist of one and only one torque pulse. Because sub-event detection is based on pre-defined voltage thresholds and/or tolerance windows, there is a possibility to erroneously actuate the anklebot, i.e., either not actuate it at all (excessively narrow band) or actuate it multiple times within the same gait cycle (excessively wide band). This measure quantifies any missed or extra sub-events within a gait cycle. For example, if a desired sub-event was not detected in one or more gait cycles,  $N_{\text{single,torque}} < N_{\text{cycle}}$  so that  $U > 0$  and similarly, if a sub-event was detected multiple times (even though it occurred only once) during a gait cycle,  $N_{\text{single,torque}} > N_{\text{cycle}}$  so that  $U < 0$ . Ideally, we desire  $U = 0$ .

Since this approach targets specific deficits of HP gait (e.g., foot drop, weak propulsion), we focus only on detecting sub-events that correspond to those deficits (e.g., toe-off, heel-off). In order to circumvent potential problems from redundant or “false” triggers for a sub-event within the

same gait cycle, a “look-no-further” criterion is embedded in the detection algorithm—that is, the first time a sub-event of interest is detected, the software program is commanded to stop the detection process for a certain period of time ( $\Delta T_{\text{sub-event}}$  ms).  $\Delta T_{\text{sub-event}}$  is determined *a priori* by averaging the sub-event duration across 10 steady-state gait cycles with the anklebot operating in a “record-only” mode. Further fine tuning of the tolerance windows and the “look-no-further” delay may be needed to accommodate changes in gait performance over the course of a training program.

2) Initiation delay ( $\Delta T$ ) is the latency between the occurrence of a sub-event and subsequent initiation of the robot-generated torque pulse. Mathematically,

$$\Delta T_{\text{avg}} = \frac{\sum_{i=1}^{N_{\text{cycle}}} (t_{i,\text{torque}} - t_{i,\text{event}})}{N_{\text{cycle}}}, \quad (2)$$

where  $\Delta T_{\text{avg}}$  (ms) is the mean delay averaged across the total number of gait cycles, and  $t_{i,\text{event}}$  (ms) and  $t_{i,\text{torque}}$  (ms) are the instants of occurrence of the event and initiation of torque in the  $i^{\text{th}}$  gait cycle, respectively. Here, initiation of robot torque is defined to be the time instant when the torque value first attains 2% of the peak torque in a given cycle. In order to prevent destabilization of the man-machine interface,  $\Delta T_{\text{avg}}$  should be “small” in some sense (e.g.,  $\Delta T_{\text{avg}} \ll T_{\text{sub-event,avg}}$ ); if not, delay compensation using one or more traditional control methods may become necessary.

## V. PHASE-SPECIFIC BIOMECHANICAL MODELS

While we may have a reliable algorithm for accurate sub-event detection that in turn precisely dictates the anklebot actuation, one still needs to determine the magnitude of robotic torques. From a clinical standpoint, this is necessary to customize robotic support to deficit severity; in control terms, this is equivalent to tuning the impedance controller gains ( $K$ ,  $b$ ) based on actual performance across training. As a first attempt, we developed simple sagittal-plane models of ankle dynamics, specific to each phase of interest (and thus key deficits). The purpose of these models is to simply approximate normative ankle dynamics for initial parameterization of the controller and hence the robot’s output during assistive walking. Moreover, the model predictions will be used to determine robotic torques over the course of training in order to modify key spatio-temporal parameters of HP gait towards more normal values as tolerated by the subject and concomitant with any gains in volitional ankle motor control and/or gait performance.

### A. Model for landing phase

A single-link<sup>1</sup> inverted pendulum (IP) model (e.g., [16]) with the rigid link acting as pivot over a moving base of support (BOS) is used to model ankle dynamics during stance, in particular, at initial contact (Fig. 4). The problem

<sup>1</sup> Here, for simplicity, the single link is considered to be a rigid inverted pendulum that includes the head-arm-trunk (HAT) plus leg, while the BOS includes foot plus ankle joint [16].

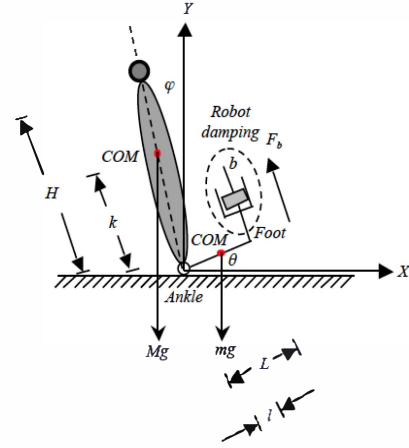


Fig. 4. Single-link IP showing heel-strike (displacement of IP from vertical is exaggerated for illustration purposes only). Robot damping lessens impact forces via resistive viscous torque at the ankle, whose magnitude is proportional to the ankle angular speed and damping.  $H$ : body height,  $M$ : body mass,  $L$ : length of foot,  $l$ : distance between ankle and foot COM,  $k$ : distance between ankle and body COM,  $b$ : robot damping,  $F_b$ : robot-generated viscous force,  $\varphi$ : angle of IP with respect to vertical,  $\theta$ : ankle angle,  $g$ : gravitational acceleration ( $9.81 \text{ ms}^{-2}$ ).

to be solved is: given a human with body height  $H$  (m) and mass  $M$  (kg), and assuming zero volitional torque<sup>2</sup> ( $\tau_h = 0 \text{ N-m}$ ), determine the minimum damping  $b_{\text{min}}$  (N-m-sec/rad) needed to constrain the peak ankle angular speed  $v_m$  (rad/s) to be less than some desired (e.g., normative) value  $V_m$  (rad/s) to lessen impact forces at landing. Mathematically,

$$b_{\text{min}} = \{b: v_m(b) \leq V_m, t_{\text{HS}} \leq t \leq t_{\text{FF}}, V_m > 0, \quad (3)$$

where  $b$  (N-m-s/rad) is the robot-induced damping (i.e., the derivative gain of the controller), and  $t_{\text{HS}}$  (s) and  $t_{\text{FF}}$  (s) represent instants of heel-strike and foot flat, respectively. In other words, we are considering the period of initial contact through mid-stance. Ignoring the foot’s mass and length relative to body mass and height, the equation of motion is:

$$I d^2\theta/dt^2 + b(d\theta/dt - v_{\text{HS}}) \cos\theta - Mgk \sin\varphi = 0, \quad (4)$$

where  $I$  is the moment of inertia ( $\text{kg-m}^2$ ),  $v_{\text{HS}}$  is the initial speed at heel-strike (rad/s),  $k$  is the distance between body center of mass (COM) and the ankle (m),  $g$  is the acceleration due to gravity ( $9.81 \text{ m-s}^{-2}$ ), and  $\varphi$  (rad) and  $\theta$  (rad) represent the IP angular position measured from vertical and the ankle angle with respect to the ground, respectively. Linearizing Eq. (4) about  $\theta = 0$  and assuming that  $|\varphi| \ll 1$  about the vertical, we obtain

$$I d^2\theta/dt^2 + b(d\theta/dt - v_{\text{HS}}) - Mgk\varphi = 0. \quad (5)$$

Equation (5) is solved for  $\dot{\theta}(t, b)$  and a desired upper-bound  $V_m$  placed on the peak speed  $v_m(b)$  i.e.,  $\|\dot{\theta}(t, b)\|_{\infty}$  i.e.,

<sup>2</sup> Clinically, a subject with lack of trace DF i.e., no palpable or observable muscle contractile activity in the gravity eliminated position.

$$0 \leq v_m(b) = v_{HS} + \frac{\alpha g M H \varphi}{b} \leq V_m, \quad t_{HS} < t \leq t_{FF}, \quad (6)$$

where  $\alpha = k/H$ . The minimum damping needed is therefore,

$$b_{\min} \geq \frac{\alpha g M H \varphi}{V_m - v_{HS}}, \quad t \in [t_{HS}, t_{FF}] \quad (\text{N-m-s/rad}). \quad (7)$$

As one would expect, the minimum damping is inversely proportional to the desired upper-bound on the peak angular speed i.e., the higher the damping, the less is the peak angular speed (and hence the impact force), and vice versa.

### B. Model for swing phase

Our objective during this phase is to provide supplemental robotic support to enable sufficient ground clearance. In other words, assuming zero voluntary ankle torque ( $\tau_h = 0$  N-m) we wish to determine the minimum stiffness  $K_{\min}$  needed for the peak ankle angle during swing to attain a desired (e.g., a more ecological) value. Mathematically,

$$K_{\min} = \{K: \theta_{\max}(K) = \gamma \theta_d, t_{TO} \leq t \leq t_{HS}\}, \quad (8)$$

where  $K$  (N-m/rad) is the robot stiffness (i.e., the proportional gain of the controller),  $\theta_d$  (rad) and  $\theta_{\max}$  (rad) are the desired and actual peak angles during swing, respectively,  $t_{TO}$  (s) is instant of toe-off so that the time period of interest  $t_{TO} \leq t < t_{HS}$  is the swing phase, and  $0 < \gamma = \theta_{\max}/\theta_d \leq 1$ . We will derive the system dynamics in the  $s$ -domain using the closed-loop transfer function (Fig. 5a) stimulated with a “ramp up - hold ramp down” reference trajectory (Fig. 5b,c):

$$\begin{aligned} \theta^*(t) = & \frac{\theta_d}{T} t \{u(t) + u(t - t_h - 2T)\} \\ & + \theta_d \left(1 - \frac{1}{T}\right) u(t - t_h) + \theta_d \left(1 - \frac{t}{T}\right) u(t - t_h - T) \end{aligned}$$

where  $T$  (sec) is the ramp duration to the desired peak angle  $\theta_d$  (rad). Ignoring the foot length for simplicity, and assuming  $t_h \ll T \ll 1$  and a [0/1] Pade' approximant for  $e^{-Ts}$ , the ankle trajectory in the  $s$ -domain is obtained, i.e.,

$$\theta(s) = \frac{\theta_d (bs + K)}{s(Ts + 1)(I_h s^2 + (b + b_h)s + (K + K_h))}, \quad (9)$$

where  $I_h$  is the ankle moment of inertia ( $\text{kg-m}^2$ ), and  $K_h$  (N-m/rad) and  $b_h$  (N-m-s/rad) are the intrinsic stiffness and damping of the ankle in DF, respectively. It can be verified from Eq. (9) that the closed-loop is Hurwitz stable since the poles satisfy  $\text{Re}[s] \leq 0$  for all  $K \geq 0$ . Taking the inverse Laplace transform of Eq. (9) yields the swing trajectory  $\theta(t)$ :

$$\theta(t) \approx \frac{\theta_d K}{(K + K_h)} (1 - e^{-\omega_n \zeta t} \cos(\omega_n \sqrt{1 - \zeta^2} \cdot t)) \quad (\text{rad}), \quad (10)$$

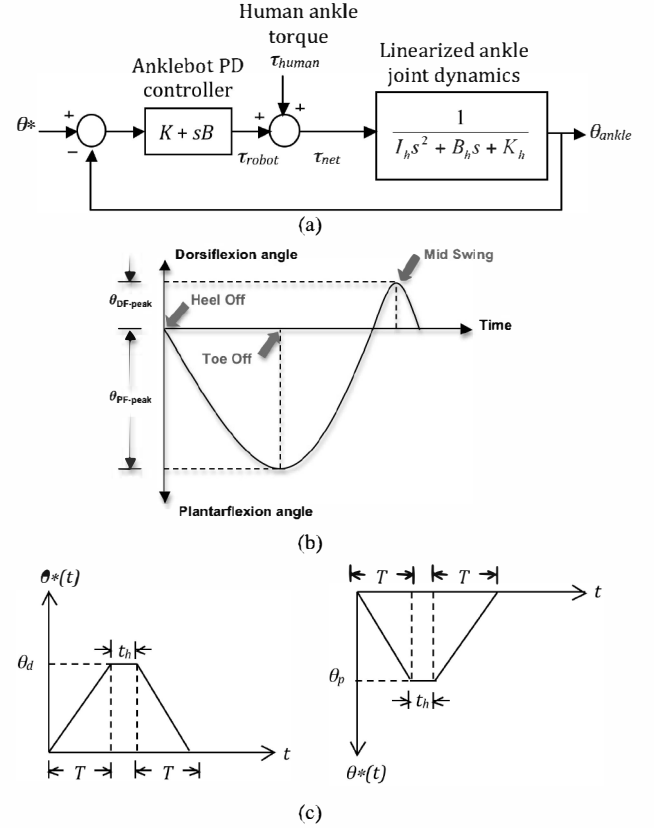


Fig. 5. (a) Block diagram of anklebot control system [3] showing major components: the PD controller parameters ( $K$ ,  $B$ ), linearized second-order ankle dynamics, and the kinematic reference. The sensor “event switch” is not shown and unity feedback is assumed; (b) Positional reference trajectory  $\theta^*$  that can be shaped using a few spatio-temporal parameters. Although the figure shows a continuous sinusoid-like waveform, in practice they are used as two distinct reference trajectories: one for PF assist and the other for DF assist; (c) The “ramp up-hold-ramp down” positional trajectory approximating the DF and PF waveforms (b). It is synthesized using three parameters ( $T$ ,  $t_h$ ,  $\theta_d$ ). For “small” ramp period  $T$ , the waveform reduces to a unit step signal ( $T \leq t \leq T + t_h$ ).

where  $\omega_n$  (rad/s) and  $0 < \zeta \leq 1$  are the system natural frequency and damping coefficient that depend solely on the intrinsic ankle properties ( $I_h$ ,  $K_h$ , and  $b_h$ ), i.e.,  $\omega_n = \sqrt{(K + K_h)/I}$  rad/s and  $\zeta = (b + b_h)/2\sqrt{I(K + K_h)}$ . To evaluate the peak swing angle, we compute  $\|\theta(t, K)\|_{\infty}$  from Eq. (10) and set it equal to  $\gamma \theta_d$ , yielding:

$$K_{\min} = \gamma K_h / (1 - \gamma), \quad t \in [t_{TO}, t_{HS}] \quad (\text{N-m/rad}). \quad (11)$$

As one would expect, the  $K_{\min}$  is inversely proportional to  $1/\gamma$  i.e., greater swing clearance necessitates higher robot stiffness, and vice versa. Moreover, the model correctly predicts less robot torque (i.e., lower  $K_{\min}$ ) for a more compliant ankle (i.e., lower  $K_h$ ), and vice versa. Unlike the model for the landing phase (Eq. (7)), the output of the swing phase model (i.e., minimum robot stiffness ( $K_{\min}$ ) needed for desired swing clearance) does not depend on whole-body parameters (body mass and height), but rather

only on the intrinsic stiffness of the paretic ankle,  $K_h$  (Fig. 6) that can be measured using experimental procedures described in [11].

We have incorporated the capability to manually adjust the ramp up - hold ramp down parameters  $\theta_d$ ,  $T$ , and  $t_h$ , and thus  $K_{min}$ , in real-time, i.e., during assisted gait, so that the therapist can set them based on actual observation of the HP gait deficits, recovery and/or compensatory strategies.

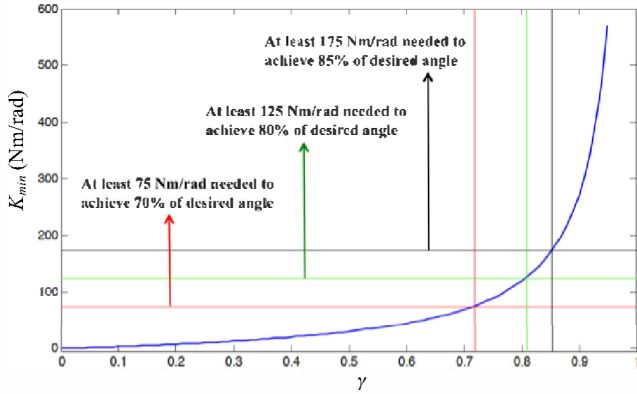


Fig. 6. Model predictions on the minimum robot stiffnesses  $K_{min}$  needed for peak swing angles to achieve different values of desired angles plotted as a function of  $\gamma$  with  $K_h = 30$  N-m/rad (see RESULTS for details).

### C. Gait deficit-adjusted controller tuning

The derived biomechanical models inform us of the controller parameter ( $K$  and/or  $b$ ) limits that are needed to target an impairment specific to that phase, i.e., Eq. (7) for ecological landing and Eq. (11) for swing clearance. This yields a centerpiece of our work: a deficit-based map in the controller parameter, i.e., a  $K$ - $b$  plane that informs us of the robot (controller) parameters needed to target and alleviate one or both of these deficits during assisted walking. This is a first step toward implementing deficit-adjusted (i.e., where one deficit is more pronounced than another) customizability of anklebot therapy to individual HP gait profiles.

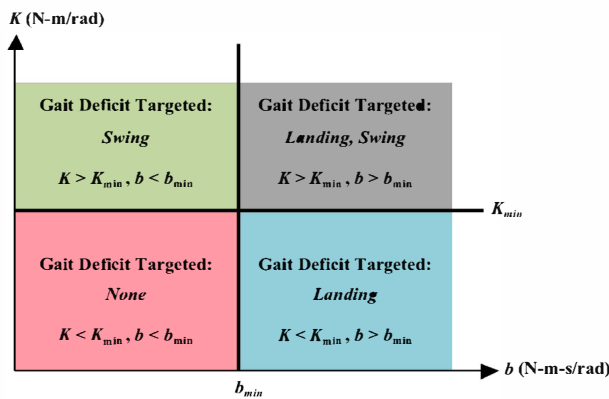


Fig. 7. A deficit-adjusted map in the controller parameter ( $K$ - $b$ ) plane. Depending on the gait deficit, the limits of  $K$  and/or  $b$  that determine the level of robotic support can be chosen using this map. The lower limits,  $K_{min}$  and  $b_{min}$ , are determined using Eqs. (7) and (11), respectively. (Top, left) Swing clearance; (Top, right) Both ecological landing and swing clearance; (Bottom, right) Ecological landing.

## VI. RESULTS

In the early phase of this study, we are testing the feasibility of our approach. Here as proof of concept, we present data from 2 participants. First, a 40-year old healthy individual who imitated HP gait and, in particular, foot drop during unassisted vs. assisted TM gait. The data from this person were used to: a) quantify the precision of footswitches in detection of gait sub-events and determine whether that information correctly actuated the anklebot, and b) validate the landing and swing phase models. Our second participant was a chronic stroke survivor with pronounced foot drop. The data from this person were used to provide initial evidence of causality of our deficit-adjusted approach in that, whether a) a few sessions of anklebot-assisted TM gait training that targets foot drop elicits gains in the peak swing angle during unassisted TM walking, and b) if there are short-term and across training retention in those gains. The protocol was approved by the University of Maryland Baltimore Institutional Review Board, the Baltimore VA R&D Committee, and MIT COUHES. Both participants gave informed consent prior to participation.

### A. Accuracy of event-triggered actuation

The healthy participant walked at a self-selected comfortable speed on the TM, first without anklebot assistance, then followed by the anklebot assisting in swing phase. For both conditions the subject was asked to keep her foot relaxed and let it “dangle” following toe-off (but with sufficient hip and knee flexion to avoid scuffing) so as to imitate foot drop and minimize any volitional torque, thereby making the experimental condition consistent with the assumption made in the models, i.e.,  $\tau_h = 0$  (N-m) in Eqs. (7) and (11). During unassisted gait, the anklebot was in a record-only mode and data from this trial was used to compute footswitch thresholds for each sub-event, that were then used to actuate the anklebot during assisted walking.

1) *Thresholds*: Validation of footswitch voltages was performed for four sub-events: toe-off, heel-strike, heel-off, and foot-flat during unassisted TM walking. Specifically, we computed the error between the actual versus theoretical (manufacturer-specified) voltage threshold for each sub-event (Table I). The errors were of the order of  $10$ - $10^2$  mV depending on the sub-event. In particular, it was very small for the heel-off and foot-flat (0.1% and 0.7% relative error, respectively) but higher for heel-strike (12%). Errors may have resulted from the movement of foot (and hence the footswitch) within the shoe itself and can be compensated for by setting tolerance bands around the voltage threshold.

TABLE I  
VALIDATION OF FOOT SWITCH OUTPUTS

Event	Measured, mV	Theoretical, mV	$\Delta$ , mV (%)
Toe-off	107-110	0.00	107-110
Heel strike	897-899	800	97-99 (12%)
Heel off	699-700	700	0-1 (0.1%)
Foot flat	1489-1491	1500	9-11 (0.7%)

2) *Timing*: After the correct thresholds were obtained, we needed to verify if: a) footswitches were accurately detecting sub-events and doing so consistently across gait cycles; and 2) in response to sub-event detection, the anklebot was being actuated accurately. Our findings were that: a) there was one and only one torque pulse for each toe-off (i.e.,  $U = 0$ ); b) the torques were initiated almost simultaneously ( $\Delta T = 9.1 \pm 0.6$  ms) with the detection of toe-off (Fig. 8).

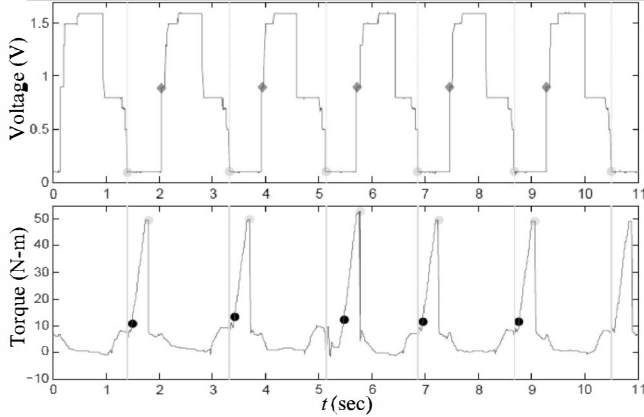


Fig. 8. Five cycles of assisted TM gait: (a) Footswitch trace during (circles: toe-off, diamonds: heel-strike); (b) Robot torques (dark circles: instant of torque initiation, light circles: peak torque). The anklebot delivered DF torques during swing, starting at toe-off.

### B. Model validation

After verifying that the sub-event detection and anklebot actuation were robustly precise, the next step was to validate the swing and landing phase biomechanical models.

1) *Swing phase*: During assisted TM walking, a peak DF angle of  $5^\circ$  was commanded with actuation starting at toe-off. Specifically, the objective was to provide robotic assistance needed for the ankle to not only cross the neutral angle during swing but, in fact, attain 70% (chosen arbitrarily) of the desired value (i.e.,  $3.5^\circ$ ). The passive ankle stiffness was estimated using prior experimental procedures ( $K_h = 30$  N-m/rad) [11]. Using  $\gamma = 0.7$  in Eq. (11), the model predicted  $K_{min} = 70$  N-m/rad. Figure 9 shows 6 gait cycles with (70 N-m/rad) and without (0 N-m/rad) robot assistance. During assisted walking, the ankle crossed the neutral in each cycle ( $3.2 \pm 0.6^\circ$ ) but not without assistance ( $-2.4 \pm 1.6^\circ$ ). The average peak swing angle ( $3.2^\circ$ ) was remarkably close to the desired value ( $3.5^\circ$ ).

2) *Landing phase*: For this test, the participant was asked to “slap” her robot-donned foot “as hard as possible” with the heel in contact with the BOS so as to simulate foot slap. The anklebot generated restorative torques at different levels of damping (0, 3, 5 N-m-s/rad). To validate the model, we imposed an arbitrary upper-bound (200°/s) on the peak angular speed during the period of initial contact through flat foot. Using the appropriate constants ( $M = 80$  kg,  $H = 1.74$  m,  $\varphi = 0.01$  rad, and  $\alpha = 0.7$  [16]) in Eq. (7), the predicted minimum damping was  $b_{min} = 3.01$  N-m-s/rad as compared to the experimental value of 3 N-m-s/rad (Fig. 10).

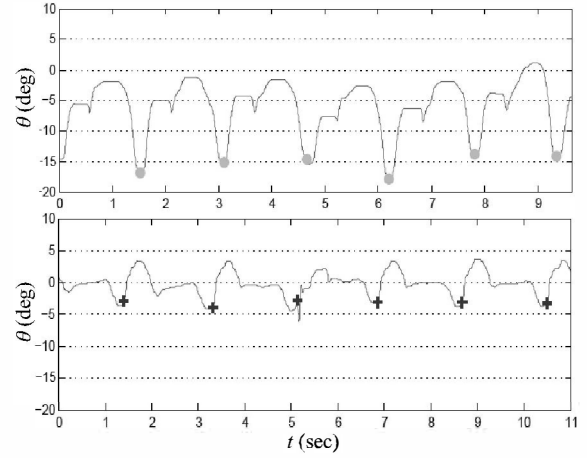


Fig. 9. Validation of swing phase model using data from a healthy subject imitating drop foot. (Top) Trace of ankle angle without robotic assistance and (Bottom) With robotic assistance, during the swing phase. The anklebot delivered DF assist following toe-off (unassisted: circles, assisted: squares). Using  $K \geq K_{min}$ , the ankle crosses the neutral into DF during swing attaining a peak value close to the desired peak angle.

### C. Proof-of-concept: Data from stroke survivor

The participant with stroke had pronounced foot drop ( $< 2^\circ$  volitional DF) making that a logical target for intervention. Training was conducted during 3xweekly visits with 48 hours between visits (M-W-F). On each visit, the session began with TM walking at self-selected speed (visit 1: 30 cm/s, visit 4: 36 cm/s) with the robot donned but not providing any assistance. This was followed by two 20-min trials of anklebot-assisted walking during which the anklebot provided swing assistance using a commanded DF reference (Fig. 5c). To ensure safety, a support harness was worn, with easy access to an emergency stop switch, and two human “spotters” were present on either side. Footswitch voltage thresholds for each sub-event were verified and if needed, adjusted on each visit to account for any inter-visit variability. The controller gains were set initially using Eq. (11) ( $\gamma = 0.75$ ,  $K_h = 50$  N-m/rad,  $\theta_d = 20^\circ$ ,  $K_{min} = 150$  N-m/rad,  $b = 1.5$  N-m-s/rad) and adjusted across visits based

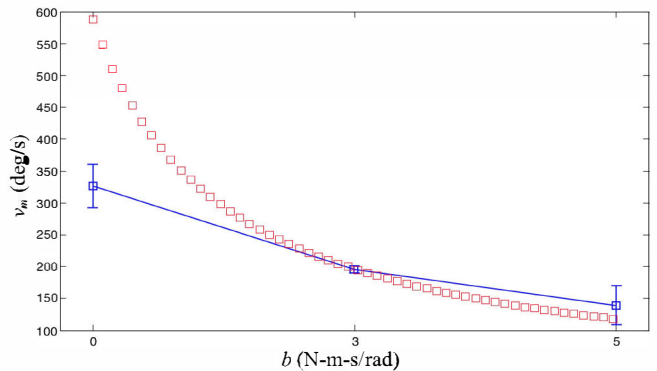


Fig. 10. Validation of landing phase model. The figure shows the predicted (open squares) and actual (mean $\pm$ SD) peak angular speed during simulated “foot slap” at different levels of robot damping. The anklebot provides restorative torque to lessen the angular speed (and hence impact force) at initial contact. Note the excellent match between the experimental and model for  $b_{min} > \sim 2$  N-m-s/rad.

on participant feedback and clinician observations during assisted walking, as well as prior performance. We compared the peak swing angle during unassisted trials conducted on the first (“pre”) visit and after 3 (“post”) training visits (Fig. 11). There was a 200% increase in the pre-post peak swing angle ( $2.5 \pm 1.1^\circ$  vs.  $7.6 \pm 0.8^\circ$ ), and these gains were of similar magnitude after completion of training at 6 weeks ( $7 \pm 0.5^\circ$ ) and notably, retained at 6-week follow-up ( $8 \pm 0.8^\circ$ ) demonstrating initial efficacy of the approach.

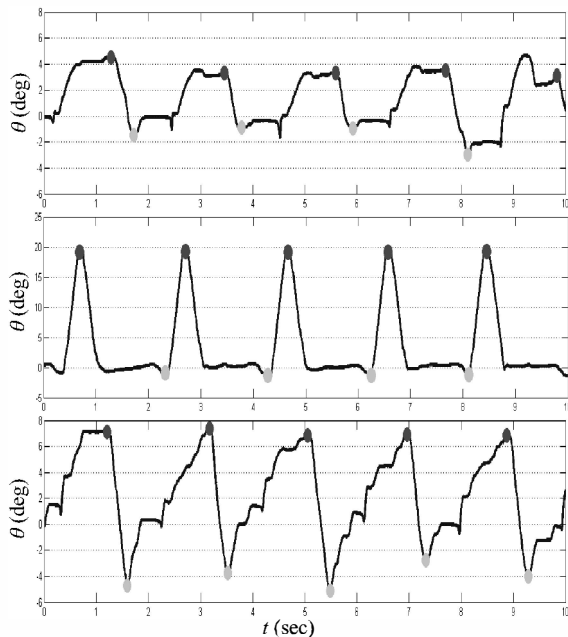


Fig. 11. Parietic ankle angular data from the participant with stroke subject showing 5 cycles of TM gait on the first visit (*Top*) Without assistance, (*Middle*) With swing assistance, commencing at toe-off (circles). The peak swing angle was close to the desired value ( $20^\circ$ ) in each gait cycle during the assisted trials thus realizing the commanded reference; (*Bottom*) Without assistance after 3 sessions. The peak swing angle (top circles) showed a marked increase after just 3 training sessions. Note difference in the Y-axis scale between assisted vs. unassisted trials.

## VII. CONCLUSIONS AND FUTURE DIRECTIONS

Here we presented a sub-task controlled, deficit-adjusted approach for anklebot-assisted gait training. The approach used thus far represents a simple but versatile approach to calibrate and control the anklebot during assisted walking: a) it can precisely time robotic support to HP gait in a way that accounts for dynamic step-to-step variability—a critical safety factor to prevent destabilization, while targeting different deficits across patients to customize locomotor training. The latter is facilitated by sagittal-plane models capable of predicting a reasonable initial value for training inputs needed to parameterize anklebot outputs to individual HP deficits during assisted gait; b) the contralateral foot can be used to establish sub-events when the ipsilateral foot is incapable of providing accurate information. We recognize, though, that additional information may be needed for this purpose—and hence have built the capacity to actuate the anklebot using the parietic knee angle information; and c) the commanded kinematics can be shaped “on-the fly”.

Initial validation tests verified that robotic support could be precisely and consistently timed to occurrence of sub-events, and that the models accurately predicted robotic support as per the specific nature of the deficit. Data from a chronic stroke survivor with drop foot showed that anklebot-assisted gait training progressively and significantly reduced foot drop after 6 weeks. We expect that over time, this approach will “teach” the central nervous system to take over from gradual withdrawal of robotic support in order to supplant the robot with volitional movements i.e., avoid “learned nonuse” of the parietic ankle. Data from a larger sample with varying gait deficits will further inform of the efficacy of the proposed approach. Future work will include: a) a model for assisted TS push-off propulsion dynamics, b) an Internal Model-based [17] adaptive controller for automatic in-course adjustment of training inputs, and c) testing efficacy of the approach for assisted OG gait.

## REFERENCES

- [1] Heart disease and stroke statistics: American Heart Association; 2009. Available from: [www.americanheart.org/statistics](http://www.americanheart.org/statistics).
- [2] A. Forster and J. Young, “Incidence and consequences of falls due to stroke: A systematic inquiry,” *BMJ*, vol. 311, pp. 83-6, 1995.
- [3] A. Roy, H.I. Krebs, D.J. Williams, C.T. Bever, L.W. Forrester, R.F. Macko, and N. Hogan, “Robot-aided neurorehabilitation: A novel robot for ankle rehabilitation,” *IEEE T Rob*, vol. 25, pp. 569-82, 2009.
- [4] R. F Macko, G. V Smith, C. L Dobrovolsky, J. D Sorkin, A. P Goldberg, and K. H Silver, “Treadmill training improves fitness and ambulatory function in chronic stroke patients,” *Stroke*, vol. 36, pp. 2206-11, 2005.
- [5] S. Jezernik, G. Colombo, T. Keller, H. Frueh, M. Morari, “Robotic orthosis Lokomat: A research and rehabilitation tool,” *NeuroMod*, vol. 6, pp. 108-115 2003.
- [6] S. Hesse and D. Uhlenbrock, “A mechanized gait trainer for restoration of gait,” *J Rehabil Res Dev*, vol. 37, pp. 701-08, 2000.
- [7] H. Schmidt, “HapticWalker—A novel haptic device for walking simulation,” In: *Proc EuroHaptics*, Munich, Germany 2004, pp. 60-7.
- [8] R. Ekkelenkamp, J. Veneman, and J. van der kooij, “LOPES: a lower extremity powered exoskeleton,” In: *Proc IEEE Int Conf Robotics Automation*, Roma, Italy 2007, pp. 3132-33.
- [9] C. J. Boserker and H. I. Krebs, “MIT-Skywalker,” In: *Proc IEEE Int Conf Rehab Robotics*, Kyoto, Japan 2009, pp. 542-9.
- [10] I. Khanna, A. Roy, M.M. Rodgers, H.I. Krebs, R.F. Macko, and L.W. Forrester, “Effects of unilateral robotic limb loading on gait characteristics in subjects with chronic stroke,” *J NeuroEng Rehab*, 7:23, 2010.
- [11] A. Roy, H.I. Krebs, C.T. Bever, L.W. Forrester, R.F. Macko, and N. Hogan, “Measurement of passive ankle stiffness in subjects with chronic hemiparesis using a novel ankle robot,” *J Neurophysiol*, vol. 105, pp. 2312-49, 2011.
- [12] A. Roy, L.W. Forrester, and R.F. Macko, “Short-term ankle motor performance with ankle robotics training in chronic hemiparetic stroke,” *J Rehabil Res Dev*, vol. 48, pp. 417-30, 2011.
- [13] L.W. Forrester, A. Roy, H.I. Krebs, and R.F. Macko, “Ankle Training With a Robotic Device Improves Hemiparetic Gait After a Stroke,” *Neurorehabil Neural Repair*, vol. 25, pp. 369-77, 2011.
- [14] T.G Hornby, D.D Campbell, J.H. Kahn, et al. “Enhanced gait-related improvements after therapist- versus robotic-assisted locomotor training in subjects with chronic stroke: a randomized controlled study,” *Stroke*, vol. 39, pp. 1786-92, 2008.
- [15] D.Y Li, A. Becker, K.A Shorter, T. Bretl, and E.T. Hsiao-Weckler, “Estimating System State During Human Walking With a Powered Ankle-Foot Orthosis,” *IEEE/ASME T Mech*, vol. 16, pp. 835-44.
- [16] K. Iqbal and A. Roy, “Stabilizing PID Controllers for a Single-Link Biomechanical Model With Position, Velocity, and Force Feedback,” *J Biomech Eng*, vol. 126, pp. 838-43, 2004.
- [17] R. Shadmehr and S. Wise, “A Computational Neurobiology of Reaching and Pointing”, MIT Press, Cambridge, MA, 2005, 20-22.